Proceedings of the ASME 2018 Internal Combustion Fall Technical Conference
ICEF2018
November 4-7, 2018, San Diego, CA, USA

ICEF2018-9545

INTEGRATION OF PRINTED SENSORS IN PLAIN ENGINE BEARINGS

Dr Roger Gorges
MAHLE Engine Systems
Rugby, UK

William Bisgrove
MAHLE Engine Systems
Rugby, UK

Ryan Curtis
MAHLE Engine Systems
Rugby, UK

Jeff Carter
MAHLE Engine Systems
Rugby, UK

James W. George
MAHLE Engine Systems
Rugby, UK

Jonathan Ritchie
MAHLE Engine Systems
Rugby, UK

Dr. Ingo Wirth
Fraunhofer IFAM
Bremen, Germany

Dr. Volker Zollmer
Fraunhofer IFAM
Bremen, Germany

Tim Rusch
Fraunhofer IFAM
Bremen, Germany

Abstract

The integration of sensors in engine components has been a long-standing wish of engine manufacturers and researchers. Conventional probes are particularly difficult to mount in moving engine parts and require time-intensive and costly preparation, while often still not reaching the site of interest close enough. The advances recently made in the field of printed electronics enable new possibilities for sensor integration that previously were not possible. Particularly, crankshaft engine bearings are an interesting component to apply those new sensors to.

An important enabling factor for the successful sensor integration has been the increasing market penetration of polymer overlays for crankshaft bearings. The driving force behind this development was the pressure from legislation to reduce CO_2 emissions, which in turn brought about new technologies such as start-stop and mild hybrids. Engine components now have to operate in much more aggressive environments, which in many cases only polymer overlays withstand. The unique application process of those coatings together with their material properties, such as robustness and non-conductivity, now allow embedding of electronic components right at the running surface of the bearings.

This paper details the development of a printed sensor that has been integrated into the bearing polymer overlay coating. Various results from respective rig testing of the sensor feedback throughout different load and speed conditions during operation are reported.

Introduction

It has been witnessed that bearing operating environments are becoming more aggressive as there is a trend for manufactures to adopt various technologies and strategies such as start stop / hybrid systems, downsizing and low viscosity oils in an effort to improve fuel consumption and reduce emission output [1]. This has given rise to the development and success of polymeric overlays that are able to withstand the ever demanding environments bearings are required to operate in. The Mahle polymer overlay is applied with a spray process in a series of layers to provide even coverage across the running surface. The benefits of using polymer overlays is well documented, furthermore the polymer possess attributes that are not available with conventional metallic overlays. The polymer is electrically insulating which, combined with the versatile application process, makes it unique in enabling integration with new technologies such as Aerosol Jet printing.

Aerosol Jet printing is a unique CAD driven, Digital Manufacturing technique for creating miniaturized electronic circuits and components [2]. Given a suitable substrate, the process is capable of printing a wide range of materials to produce complicated three dimensional electronic circuits on shaped surfaces. The Aerosol Jet printing process finely atomizes the functional ink and dispenses it onto the target substrate; the process is described by Figure 1.

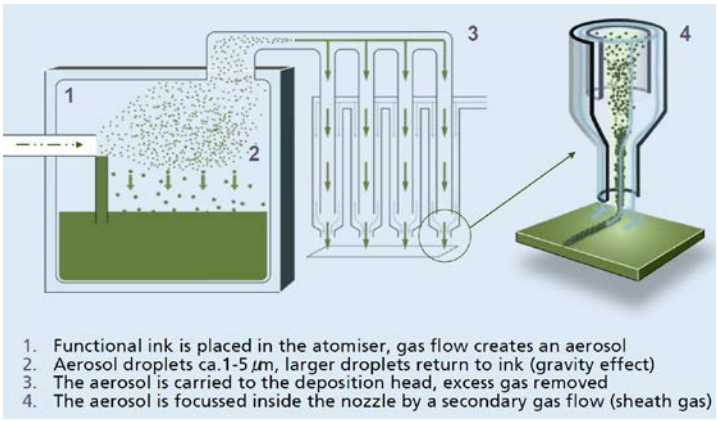

Figure 1: Schematic of Aerosol Jet printing process (adapted from [2]).

Once the ink has been printed onto the target substrate the final step in the process is to sinter the ink to form the conductive printed structure.

Knowledge of the engine operating conditions is crucial in the successful development of new products and their longevity in the field. Historically engine development has relied on the use of conventional probes that can rarely reach the site of interest, with the key locations either being hard to reach or requiring telemetric data transfer. With the success of polymer overlays and the proliferation of Aerosol Jet printing this new sensor technology has now become ready for transfer from academia into industry.

The development of sensors that can be integrated into the bearing overlay can provide a key insight into real operating environments, which at present is only available through numerical simulations.

Sensor Development

The development of the integrated sensors began with simple Ag (Silver) printed circuits. The initial challenge was not only to print the circuit onto the inner diameter of the bearing but also maintain electrical insulation from the conductive substrate material. This was achieved by applying a Si-based insulating layer to the bearing prior to printing via a PVD (physical vapor deposition) process. Although this achieved the necessary insulation it also resulted in a significant lack of adhesion when applying the polymer overlay.

MAHLE's series polymer overlay contains Al (Aluminum) flakes; however it does also possess good insulating qualities. This is a consequence of the Al flakes themselves being encased within the insulating polymer. The polymer spraying process was modified to apply an initial layer of polymer to the bearing prior to printing to insulate the print from the conductive metallic bearing substrate. To facilitate the success of the Aerosol Jet printing process, the polymer undergoes a surface activation phase to achieve the most suitable surface properties prior to printing. Once printing of the sensor is complete the remaining polymer coat is applied on top of the sensor. This fully encases the printed circuit within the polymer overlay and results in good polymer adhesion, as shown in Figure 2.

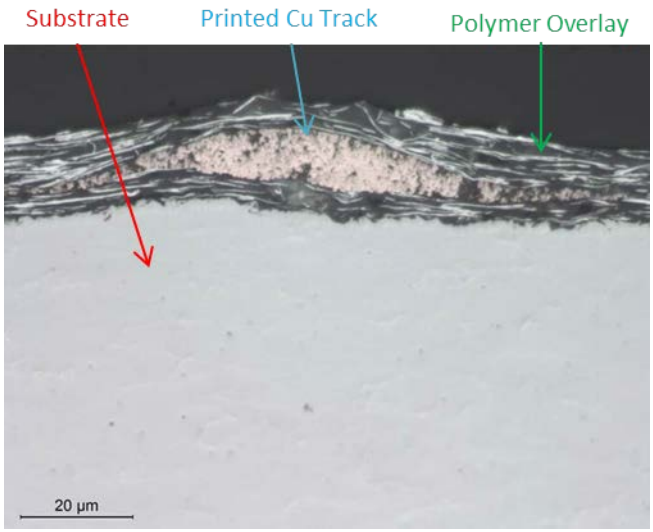

Figure 2: Printed circuit within the polymer overlay.

With the polymer confirmed as a satisfactory insulation layer, the development of a functional temperature sensor commenced. Using the same Aerosol Jet printing method a thermocouple was created. To produce a thermocouple the printed circuit was separated into two individual tracks that intersect. The tracks are printed in Cu (Copper) and CuNi (Copper Nickel) respectively and are approximately 100μm wide and 8μm high. The intersection of these two materials creates a T-Type thermocouple junction as shown in Figure 3.

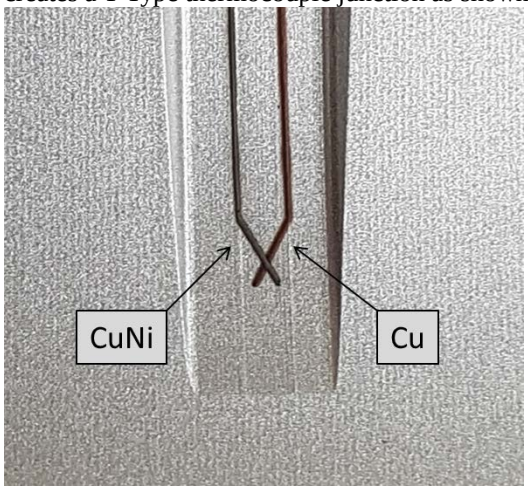

Figure 3: Printed Cu/CuNi T-type TC.

The combustion engine is an extremely unforgiving environment particularly for a printed circuit. The polymer protects the printed circuit from abrasive wear, oil, corrosion and other chemical interactions that may occur, however a further step was taken to defend the printed circuit and

connection method; the addition of a partial groove. The main purpose of the groove is to house the connector however it can also be used to control the amount of sensitivity required from the sensor versus the length of the printed circuit. This is best described by Figure 4.

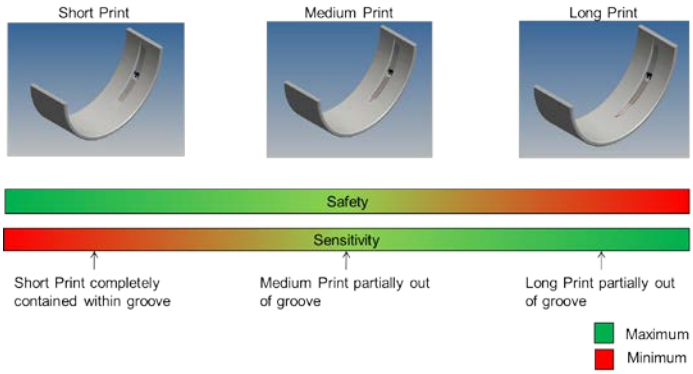

Figure 4: Print length vs. sensitivity.

The groove allows different printing options, from printing entirely within the relative safety of the groove at the cost of sensitivity to printing directly up to the site of interest for maximum sensitivity but with the associated risk of leaving the protection of the groove.

Functional Testing

Thermal Cycling

Thermal cycling of the printed sensors was carried out in a test oven to ensure the accuracy of the sensor was equivalent to a conventional T-Type TC. Bearings with printed TC's were assessed both before and after the final polymer coat; this ensured there was no detriment to the sensor accuracy as a result of the polymer coating. The printed TC's were compared to a conventional TC bonded to the surface of a polymer coated bearing. The results of the test are illustrated by Figure 5.

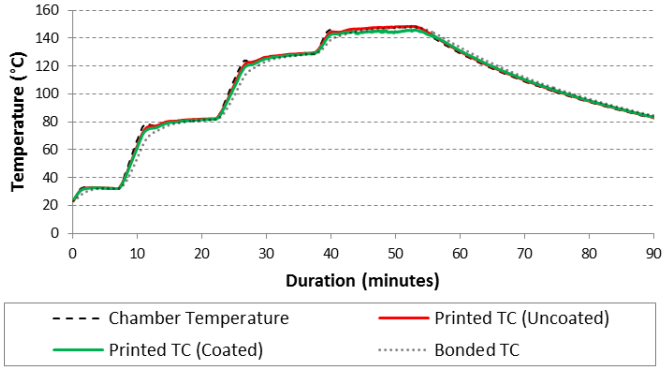

Figure 5: Thermal cycling test temperature response.

The air temperature in the oven increases from 30°C to 150°C with the maximum difference between the polymer coated TC and the conventional TC at 150°C of less than 1.5K. It is also noted that the printed TCs respond faster and closer to the air temperature than the conventional TC.

Rig Testing

All rig testing was conducted using a modified Sapphire test rig. The Sapphire rig applies a load via an eccentric shaft and a hydraulic ram to simulate the force applied by a typical combustion engine. A schematic of the Sapphire test rig is shown in Figure 6.

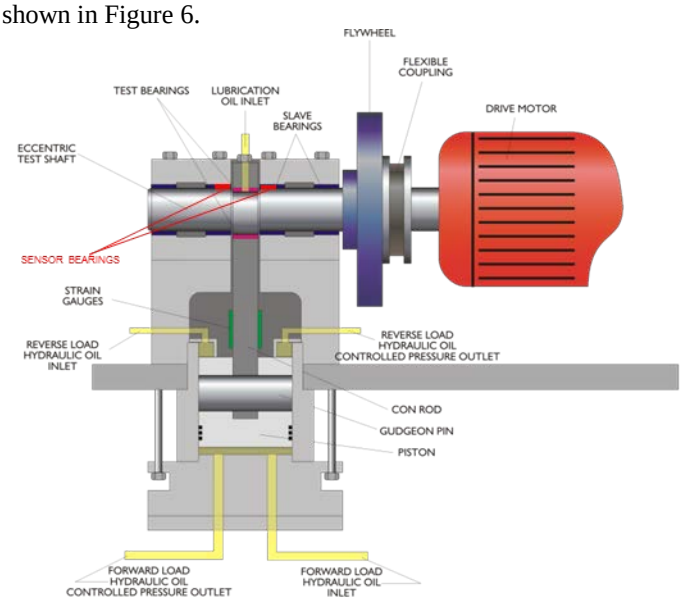

Figure 6: Sapphire test rig schematic.

The Sapphire comprises an electric motor that drives a test shaft that is concentrically mounted by a set of slave bearings. The center of the test shaft is eccentric to the slave bearing journals. Typically, the test bearing is mounted around the eccentric part of the shaft in the test housing. The test housing is connected to the hydraulic piston via a connecting rod. The rotation of the test shaft causes the piston to reciprocate. Hydraulic pressure is applied to either side of the piston, as the piston moves into the hydraulic pressure a cyclic force is generated. The hydraulic pressure in the cylinder is controlled, thus controlling the force generated and the maximum specific load applied to the bearing. The force is measured by a strain gauge attached to the connecting rod. A typical Sapphire load curve is show in Figure 7. The Sapphire has an automated control system, which enables any desired load and speed combination.

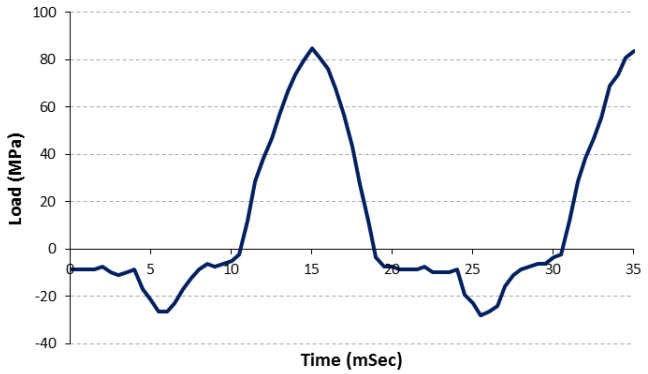

Figure 7: Sapphire load curve.

In order to test the printed thermocouples in a main bearing configuration, the rig was modified to house the sensor bearings in the slave locations; this is shown in Figure 6. It was assumed that the force measured at the connecting rod is split evenly between the two tested bearings.

The test rig was programmed with a test cycle that simultaneously increments the load and speed from 800RPM to 3000RPM, where the load is then reduced irrespective of the shaft speed. The load and speed is then incrementally reduced back to 800RPM. The cycle is shown in Figure 8. This test was repeated twice; first with an oil feed temperature of 80°C, then with an oil feed temperature of 100°C. The general test parameters are shown below in Table 1.

Table 1: Test parameters.

Test Parameter	Value
Shaft Material	Hardened Steel
Surface Roughness	<0.2Ra
Shaft Speed	800 – 3000RPM
Test Load	20 – 60MPa
Lubricant Oil	Synthetic 46
Oil Feed Temperature	80 – 100°C

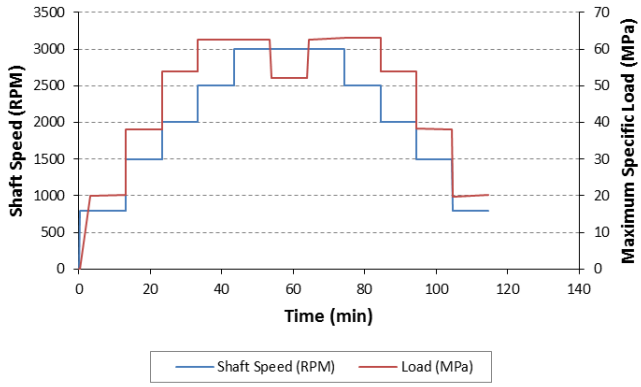

Figure 8: Programmed Sapphire test cycle.

The result of the test cycle is displayed in Figure 9. To simplify the chart the load and speed has been combined to show peak PV (pressure velocity).

The response from the printed sensor has a clear correlation with the change in peak PV. The sensor detects the change in bearing temperature as a result of the change in the operating environment. The response from the sensor throughout the test at the different oil feed temperatures is fairly parallel, indicating that the relationship between the change in bearing running temperature and the change in PV is independent of oil feed temperature.

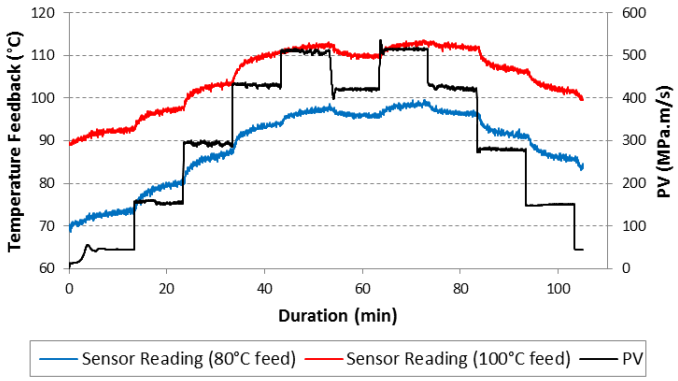

Figure 9: PV over test duration for 80°C vs 100°C oil feed temperature.

Having confirmed the printed sensor was capable of detecting bearing temperature changes as a results of changes in peak PV, further tests were conducted to assess the sensors ability to detect changes in the bearing operation when a known fault was introduced into the system.

One of the sensor bearings was installed into a defective housing and another into a faultless housing. The defective housing is 249µm out of round, due to a large deformation in the crown region. This can be seen in Figure 10.

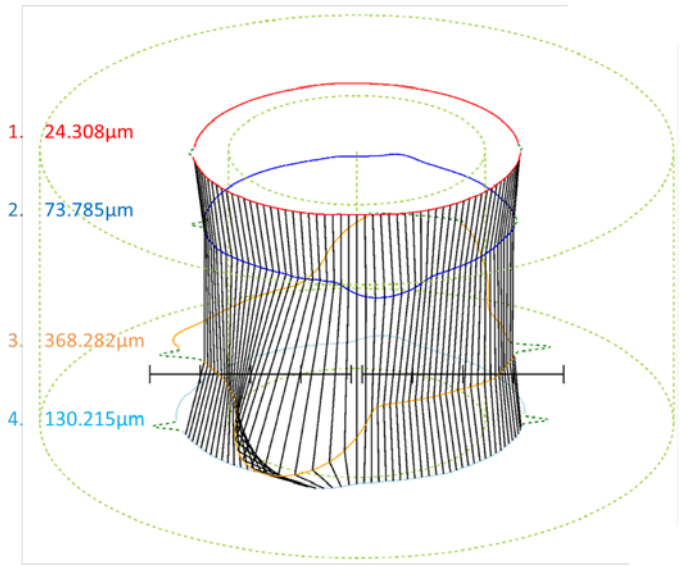

Figure 10: Roundness trace of the bearing housing.

The sensor bearing was fitted between track 3 and 4, therefore the average of these two roundness traces has been taken to give the roundness figure of 249µm out of round. Track 3 in Figure 10 shows the deformation is concentrated in the crown region of the bearing housing.

The same test procedure was executed and the response from the respective sensor bearings has been displayed against peak PV in Figure 11.

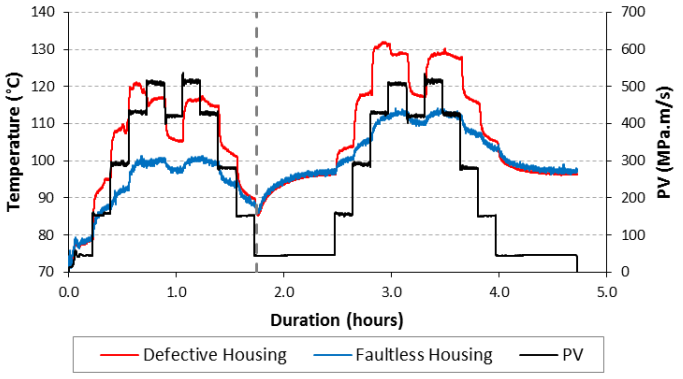

Figure 11: Bad vs good housing.

The sensor bearing in the faultless housing shows the same relationship as the previous test. However, the operating conditions observed in the defective housing are considerably different, with a much greater temperature response. The sensor bearing immediately detects the increase in bearing temperature caused by the adverse operating conditions imposed by the defective housing. The sensor feedback from the defective location quickly diverges away from the temperature of the faultless location as soon as the peak PV is increased. The bearing in the defective location consistently operates at a higher temperature than the bearing in the faultless housing. However at the end of each cycle when the PV is reduced it is noted that the temperature response from the defective location converges back in line with the running temperature of the bearing in the faultless location. This can be attributed to the polymer coatings ability to conform to the detrimental operating conditions, with the same convergence taking place at the end of both cycles.

The unfavorable conditions imposed by the housing are witnessed in the post-test visual appearance of the bearings in Figure 12. The deformation in the crown region of the defective housing has prevented effective film generation and forced the bearing into a severe contact condition, particularly at the higher load sites. The wear scar of the bearing in this location shows the conformance of the polymer to withstand the damaging conditions, in contrast to the bearing from the faultless location that remains unmodified.

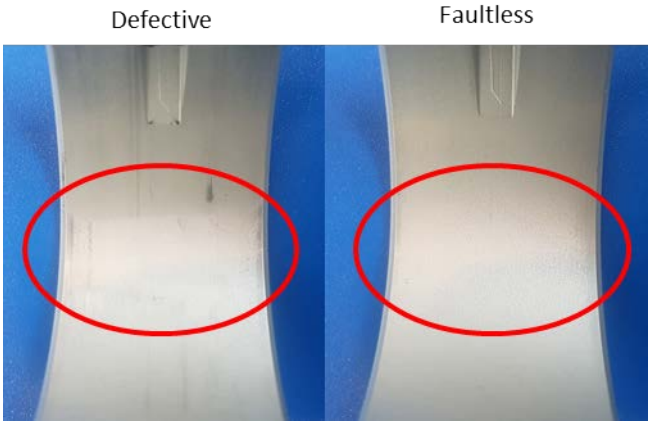

Figure 12: Post-test pictures.

The temperature response at each of the PV sites from both of the tested bearings is given in Figure 13.

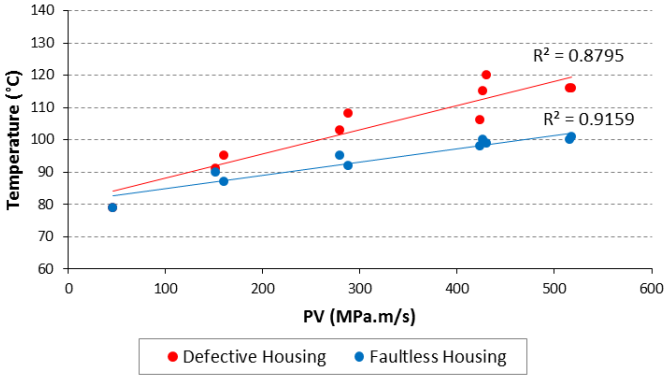

Figure 13: Temperature response vs PV.

It is noted that the correlation for the defective housing is somewhat weaker than the faultless housing; this is a consequence in part of the conforming effects of the polymer

reducing the resultant temperature of the running condition caused by the defective housing.

Conclusion

The introduction of Smart components brings with it the possibility of using the relationship between oil feed temperature, PV and bearing operating temperature to immediately determine faults in a fired engine and prevent early component failure that would otherwise result in catastrophic engine damage. This can be used particularly in the field of advanced research and development, when the running conditions can be effectively assessed to determine the consequence of altering bearing material or geometry in sensitive applications.

Other sensor possibilities also exist, one of which is a wear sensor. When printing outside of the groove the temperature sensor can also be used to detect wear of the overlay. However a standalone Ag wear sensor is also possible in the future to reduce the complexity of the printing process. Real time response from the sensor describing the condition of the bearing overlay will increase the precision of just in time servicing, enabling safe extension of the service intervals whilst minimizing the associated risk.

Outlook

The functionality of the sensor will also be demonstrated in the main bearings of an upcoming engine test. A similar cycle to the automated rig testing will be conducted, with the sensor response measured at various different load and speed conditions and then compared to simulation data. This development loop can then be used to increase the accuracy of both the printed sensor and the simulation systems, before extended durability testing of the printed sensor.

Nomenclature

Ag: Silver
Si: Silicon
Cu: Copper
CuNi: Copper Nickel
TC: Thermocouple
PVD: Physical vapor deposition
RPM: Revolutions per minute
PV: Pressure-velocity

Acknowledgements

We would like to thank James Thyer, Andreas Schilling, Craig Shorland, Richard Pool, Jack Merchant, Steve Sanders and Isaac Nielsen for their support in this complex and interdisciplinary project.

References

1. George, James and Brock, Ronald. “Polymeric Engine Bearings for Hybrid and Start Stop Applications”. SAE Technical Paper 2012-01-1966. 2012
2. Hedges. Martin and Borras Marin, Aaron. “3D Aerosol jet printing-Adding electronics functionality to RP/RM” *DDMC 2012 conference:* pp. 14-15.